ADBA Chaos and Fractals
Cutting-Edge Scientific Solutions

e-ISSN: 3023-8951
RESEARCH ARTICLE
Vol.3 / No.1 / 2026 / pp.29-37
https://doi.org/10.69882/adba.chf.2026015

Nonlinear Dynamics and Chaos Control in a Discrete Sel'kov Model with Substrate Inhibition

Ansar Abbas *,1 **and Abdul Khaliq** *,2
*Department of Mathematics, Riphah International University, Lahore Campus, Pakistan.

ABSTRACT An investigation of the dynamic effects of substrate inhibition in a modified Sel'kov model of glycolytic oscillations is presented in this paper. With a saturated nonlinear term in place of classical polynomial feedback, the discrete-time formulation captures enzymatic regulation more realistically. It exhibits complicated dynamics, including period-doubling bifurcations, compared to the classical continuous Sel'kov model, which undergoes Hopf bifurcation. In this study, the model's behavior is investigated in multiple ways, including fixed point determination, stability assessment based on the Schur-Cohn criterion, and comprehensive numerical bifurcation analysis. Dynamic transitions from stability to periodic cycles, and then to chaos are revealed. Based on a comparative analysis with the classical model, we demonstrate how substrate inhibition induces complex nonlinear behavior through successive bifurcations. A deeper understanding of feedback regulation in biochemical systems can be gained from this study.

KEYWORDS
Discrete modified Sel'kov model
Substrate inhibition
Period-doubling bifurcation
Chaos control
Comparative dynamical analysis

INTRODUCTION

In cellular metabolism, glycolytic oscillations are characterized by periodic fluctuations in the concentrations of metabolites such as nicotinamide adenine dinucleotide (NADH) and adenosine triphosphate (ATP). Originally observed in yeast, these oscillations have now been identified in a variety of cell types, including pancreatic β-cells and cardiac myocytes (Goldbeter 1996; Fall *et al.* 2002). Apart from their role in metabolism, glycolytic oscillations also play a critical role in calcium signaling, circadian rhythms, and hormone production; particularly insulin (Bertram *et al.* 2007; Gaspers and Thomas 2000; Tornheim and Lowenstein 1979). Further, dysregulation of these oscillations is associated with metabolic diseases, including diabetes and cancer (Teusink *et al.* 2000; Richard 2003).

It has proven invaluable to use simplified mathematical models to investigate such rhythmic behavior. Among the most influential is the Sel'kov model (Sel'kov 1968), which encapsulates the nonlinear feedback dynamics responsible for glycolytic oscillations. Based on this model, complex dynamic phenomena have been investigated, such as enzyme kinetics, limit cycles, and bifurcation structures. Nonlinear dynamics and bifurcation theory are used for theoretical analysis (Strogatz 2015; Wiggins 2003; Kuznetsov 2004), focusing on Hopf bifurcation Hassard *et al.* (1981), explains how steady states become sustained oscillations as system parameters change. A variety of non-equilibrium thermodynamic platforms can be applied to these methods to clarify how feedback, autocatalysis, and dissipation produce oscillations and multistability (Schnakenberg 1979; Nicolis and Prigogine 1977).

Based on the following system of ordinary differential equations, Sel'kov describes in detail the dynamics of substrate and product concentrations during the phosphofructokinase reaction (PFK) in glycolysis:

$$\left.\begin{aligned} \frac{dx}{dt} &= \alpha - x + x^2 y, \\ \frac{dy}{dt} &= \beta - x^2 y, \end{aligned}\right\} \tag{1}$$

where $x(t)$ and $y(t)$ represent the concentrations of adenosine diphosphate (ADP) and adenosine triphosphate (ATP), respectively. The parameters α and β denote the external fluxes of ADP and ATP into the system. The nonlinear term x^2y introduces an autocatalytic interaction, capturing the feedback mechanism characteristic of the glycolytic pathway, in which ADP promotes further production of ATP.

Although this model is fundamental, it ignores substrate inhibition, which reduces enzyme activity when substrate concentrations are high. Typically, this inhibitory effect occurs when excess sub-

Manuscript received: 29 October 2025,
Revised: 7 January 2026,
Accepted: 9 January 2026.

[1]kute_ansar@yahoo.com (**Corresponding author**)
[2]khaliqsyed@gmail.com

strate molecules interfere with the efficiency of enzymes through the saturating of active sites or the activation of allosteric mechanisms. This biologically relevant behavior is incorporated by modifying the autocatalytic term to a saturated, rational form $\frac{x^2y}{1+\rho x^2}$, where $\rho > 0$ is the inhibition coefficient. The modified model thus becomes:

$$\left.\begin{aligned} \frac{dx}{dt} &= \alpha - x + \frac{x^2 y}{1+\rho x^2}, \\ \frac{dy}{dt} &= \beta - \frac{x^2 y}{1+\rho x^2}. \end{aligned}\right\} \tag{2}$$

In this modification, a saturation mechanism is introduced that limits the reaction rate at high substrate concentrations, in accordance with observed enzyme kinetics (Segel 1988; Murray 2002; Hofmeyr and Cornish-Bowden 1986). In some cases, continuous-time models are not adequate for capturing biological processes that involve discrete regulatory events, sampling intervals, or digital controls. Discrete-time models are more practical and insightful in such contexts (Elaydi 2005).

By applying a forward Euler discretization with step size $h > 0$, the system can be reformulated as a nonlinear difference equation:

$$\left.\begin{aligned} x_{n+1} &= x_n + h\left(\alpha - x_n + \frac{x_n^2 y_n}{1+\rho x_n^2}\right), \\ y_{n+1} &= y_n + h\left(\beta - \frac{x_n^2 y_n}{1+\rho x_n^2}\right). \end{aligned}\right\} \tag{3}$$

This discrete formulation preserves the essential nonlinear feedback and inhibition structure of the original system while enabling the study of a wider range of dynamic phenomena, including fixed points, bifurcations, and chaotic regimes (Guckenheimer and Holmes 1983; Alligood *et al.* 1996). Discrete-time approaches are especially suitable for modeling biochemical systems with threshold effects, delay responses, and pulse-driven behaviors (Chen *et al.* 2021; Elaydi 2005). We have also been able to improve our understanding of cellular function through the integration of mathematical modeling with systems biology. With the combination of quantitative models and experimental data, quantitative models can be used to design bioreactor control strategies and predict emergent behavior in complex networks (Heinrich and Schuster 1996; Glass and Mackey 1988; Bastin and Dochain 1990). Through educational frameworks, theoretical tools have been made accessible to researchers across disciplines, facilitating the application of mathematical biology (De Vries *et al.* 2006).

By representing feedback mechanisms in enzymatic reactions, Sel'kov's classical model has long served as a foundation for understanding these oscillations. A new model has been developed to capture the complexity of behaviors observed in biological systems in recent years. According to Sataric *et al.* (2024), diffusion is implicated in inducing symmetry breaking instabilities that might result in spatial homogeneity in concentrations of metabolites. Substrate inhibition, a phenomenon that inhibits enzyme activity at excessive substrate concentrations, is another critical factor affecting glycolysis. Yoshino *et al.* (2015) developed an analytical method to determine kinetic parameters of Allee Effect in metabolic pathways, emphasizing its prevalence and regulatory significance.

Glycolytic models with substrate inhibition reveal intricate dynamic behaviors, including bifurcations due to period-doubling. In such a system, bifurcations indicate transitions from stable oscillatory states to chaotic dynamics as parameters change. An analysis by Merdan and Duman (2022) demonstrated period-doubling bifurcations in a modified discrete-time model with substrate inhibition. In addition, Gambino *et al.* (2022) suggest that discrete-time frameworks benefit understanding the richness of biological rhythms as well as their susceptibility to chaos.

It is clear that classical models need to be refined to incorporate additional biological realism, such as substrate inhibition, so that nonlinear dynamics of glycolytic oscillations can be understood better. We analyze a modified Sel'kov model that integrates substrate inhibition in this paper, examining its dynamic behavior with a bifurcation analysis and comparing it with the original model to determine how this modification affects oscillation patterns and system stability.

Our work is novel because we include substrate inhibition into a discrete-time variant of the classical Sel'kov model to enhance its biological realism. With the proposed model, a rational inhibition term is incorporated within the autocatalytic feedback mechanism, accurately representing saturation behavior at high substrate concentrations. It is particularly important in computational and experimental contexts involving sampled data to be able to analyze bifurcation structures and oscillation patterns by discretizing the modified system.

An important aspect of this study is the analysis and numerical exploration of the model's fixed points and local dynamics, with a focus on identifying bifurcation conditions. In addition, we perform a local reduction of the system near critical bifurcation points by using center manifold theory, allowing us to comprehend nonlinear behavior near stability thresholds more deeply. This work provides a novel approach to modeling enzymatic feedback with substrate inhibition in discrete-time settings, shedding new light on mechanisms governing metabolic stability and oscillations. Consequently, the inclusion of substrate inhibition allows the model to exhibit complex bifurcation and chaotic dynamics that are not captured by the classical discrete Sel'kov framework.

The objective of this study was to develop a discrete-time adaptation of the classical Sel'kov model, enhanced with saturated inhibitory feedback. The paper is organized as follows. In Section *Equilibrium Point and Stability Analysis*, we analyze the system's fixed point's existence and local stability. By employing the Schur-Cohn criterion, it is shown that a unique fixed point exists, and its stability is investigated. By implementing a state feedback control strategy, the marginal stability region associated with the chaotic behavior of System 4 has been identified, as elaborated in Section *Chaos control*. The trajectories of eigenvalues are explored in Section *Numerical Analysis*, where period-doubling bifurcations are identified, leading to the emergence of cyclic and chaotic dynamics. Section *Global Bifurcation Overview for* $\beta \in [1, 100]$ presents a comprehensive global bifurcation analysis within the interval $\beta \in [1, 100]$, highlighting the transitions between stability and periodicity. In Section *Comparative Discussion with the Classical Sel'kov Model*, we compare the classical continuous Sel'kov model with the proposed discrete model with saturated feedback in detail. A table summarizing dynamic features, bifurcation behavior, computational aspects, and biological implications is provided. To conclude, Section *Conclusion* summarizes the core analytical and numerical insights of the paper, emphasizing how discrete modeling and saturation contribute to rich dynamical phenomena in biochemical systems.

EQUILIBRIUM POINT AND STABILITY ANALYSIS

We examine the discrete-time model obtained using the forward Euler method from a biologically inspired glycolytic system with substrate inhibition. In this context, the proposed model is pre-

sented below, with the corresponding state variables and parameters detailed in Table 1.

$$\left.\begin{aligned} x_{n+1} &= x_n + h\left(\alpha - x_n + \frac{x_n^2 y_n}{1+\rho x_n^2}\right), \\ y_{n+1} &= y_n + h\left(\beta - \frac{x_n^2 y_n}{1+\rho x_n^2}\right), \end{aligned}\right\} \tag{4}$$

Table 1 State variables and parameters of the discrete model and their role

State variables	
x_n	Concentration of **ADP** (adenosine diphosphate) at discrete time step n. Contributes to glycolysis processes catalyzed by phosphofructokinase (PFK).
y_n	Concentration of **ATP** (adenosine triphosphate) at discrete time step n. Represents the reaction product.
Parameters	
α	Constant inflow or supply rate of ADP. Indicates how much substrate is being imported or produced externally.
β	Constant inflow or supply rate of ATP. Represents the baseline energy or production level at which the system operates.
ρ	Substrate inhibition coefficient. Higher values indicate stronger inhibition due to enzyme saturation at high ADP concentrations.
h	Discrete time step size. Determines the temporal resolution of the simulation in forward Euler discretization.

Existence of Fixed Points

A fixed point $(\tilde{x}, \tilde{y})$ of the system satisfies $x_{n+1} = x_n = \tilde{x}$ and $y_{n+1} = y_n = \tilde{y}$. Substituting into Eq. (4), we obtain the steady-state conditions:

$$\left.\begin{aligned} \tilde{x} &= \tilde{x} + h\left(\alpha - \tilde{x} + \frac{\tilde{x}^2\tilde{y}}{1+\rho\tilde{x}^2}\right), \\ \tilde{y} &= \tilde{y} + h\left(\beta - \frac{\tilde{x}^2\tilde{y}}{1+\rho\tilde{x}^2}\right). \end{aligned}\right\} \tag{5}$$

Subtracting $\tilde{x}$ and $\tilde{y}$ from both sides yields:

$$\left.\begin{aligned} 0 &= \alpha - \tilde{x} + \frac{\tilde{x}^2\tilde{y}}{1+\rho\tilde{x}^2}, \\ 0 &= \beta - \frac{\tilde{x}^2\tilde{y}}{1+\rho\tilde{x}^2}. \end{aligned}\right\} \tag{6}$$

From the second equation in (6), we solve for $\tilde{y}$:

$$\frac{\tilde{x}^2\tilde{y}}{1+\rho\tilde{x}^2} = \beta \quad \Rightarrow \quad \tilde{y} = \beta \cdot \frac{1+\rho\tilde{x}^2}{\tilde{x}^2}, \quad \tilde{x} \neq 0. \tag{7}$$

Substitute $\tilde{y}$ into the first equation of (6) gives:

$$0 = \alpha - \tilde{x} + \frac{\tilde{x}^2}{1+\rho\tilde{x}^2} \cdot \frac{(1+\rho\tilde{x}^2)\beta}{\tilde{x}^2} = \alpha - \tilde{x} + \beta. \tag{8}$$

Hence, we find:

$$\tilde{x} = \alpha + \beta.$$

Using this in Eq. (7), we obtain:

$$\tilde{y} = \frac{(1+\rho(\alpha+\beta)^2)\beta}{(\alpha+\beta)^2}.$$

Therefore, the system has a unique biologically meaningful fixed point $(\tilde{x}, \tilde{y})$ given by:

$$(\tilde{x}, \tilde{y}) = \left(\alpha+\beta,\ \frac{(1+\rho(\alpha+\beta)^2)\beta}{(\alpha+\beta)^2}\right). \tag{9}$$

This fixed point exists and is positive for all $\alpha, \beta > 0$ and $\rho \geq 0$, satisfying the biochemical requirement that metabolite concentrations must remain non-negative.

Stability Analysis via Schur–Cohn Conditions

To investigate the local stability of the nontrivial equilibrium point of the system, we compute the Jacobian matrix and apply the Schur–Cohn stability conditions for discrete-time two-dimensional systems. Let us define:

$$f(x,y) = x + h\left(\alpha - x + \frac{x^2 y}{1+\rho x^2}\right), \quad g(x,y) = y + h\left(\beta - \frac{x^2 y}{1+\rho x^2}\right).$$

We now compute the Jacobian matrix $\tilde{J}$:

$$J = \begin{bmatrix} \frac{\partial f}{\partial x} & \frac{\partial f}{\partial y} \\ \frac{\partial g}{\partial x} & \frac{\partial g}{\partial y} \end{bmatrix}\Bigg|_{(\tilde{x},\tilde{y})}. \tag{10}$$

Define:

$$R(x,y) = \frac{x^2 y}{1+\rho x^2}.$$

Here,

$$\frac{\partial f}{\partial x} = 1 + h\left(-1 + \frac{\partial R}{\partial x}\right), \quad \frac{\partial f}{\partial y} = h\left(\frac{\partial R}{\partial y}\right).$$

and

$$\frac{\partial g}{\partial x} = -h\left(\frac{\partial R}{\partial x}\right), \quad \frac{\partial g}{\partial y} = 1 - h\left(\frac{\partial R}{\partial y}\right).$$

Compute:

$$\frac{\partial R}{\partial x} = \frac{2xy(1+\rho x^2) - x^2 y(2\rho x)}{(1+\rho x^2)^2} = \frac{2xy(1+\rho x^2) - 2\rho x^3 y}{(1+\rho x^2)^2},$$

$$\frac{\partial R}{\partial x} = \frac{2xy(1+\rho x^2 - \rho x^2)}{(1+\rho x^2)^2} = \frac{2xy}{(1+\rho x^2)^2},$$

$$\frac{\partial R}{\partial y} = \frac{x^2}{1+\rho x^2}.$$

So the Jacobian becomes:

$$\tilde{J} = \begin{bmatrix} 1 + h\left(-1 + \frac{\partial R}{\partial x}\right) & h \cdot \frac{\partial R}{\partial y} \\ -h \cdot \frac{\partial R}{\partial x} & 1 - h \cdot \frac{\partial R}{\partial y} \end{bmatrix}.$$

Let:

$$r = \frac{\partial R}{\partial y}\Big|_{(\tilde{x},\tilde{y})} = \frac{\tilde{x}^2}{1+k\tilde{x}^2}, \quad s = \frac{\partial R}{\partial x}\Big|_{(\tilde{x},\tilde{y})} = \frac{2\tilde{x}\tilde{y}}{(1+\rho\tilde{x}^2)^2}.$$

Then:

$$\tilde{J} = \begin{bmatrix} 1 + h(-1+s) & hr \\ -hs & 1 - hr \end{bmatrix}.$$

Definition 1 (Schur-Cohn Criterion (Elaydi 2005))**.** Let J be the Jacobian matrix of a two-dimensional discrete dynamical system evaluated at a fixed point:

$$J = \begin{bmatrix} a_{11} & a_{12} \\ a_{21} & a_{22} \end{bmatrix},$$

with trace and determinant given by

$$\mathrm{tr}(J) = a_{11} + a_{22}, \quad \det(J) = a_{11}a_{22} - a_{12}a_{21}.$$

Then, the stability of the fixed point is determined by the following conditions:

- **Asymptotically Stable :** The fixed point is asymptotically stable if and only if the following three inequalities hold:

$$\begin{aligned} 1 - \mathrm{tr}(J) + \det(J) &> 0, \\ 1 + \mathrm{tr}(J) + \det(J) &> 0, \\ |\det(J)| &< 1. \end{aligned}$$

- **Unstable:** At least one of the following holds:

$$\begin{aligned} 1 - \mathrm{tr}(J) + \det(J) &< 0, \\ 1 + \mathrm{tr}(J) + \det(J) &< 0, \\ |\det(J)| &\geq 1. \end{aligned}$$

- **Borderline Cases (Bifurcations May Occur):** Fixed point lies on the boundary of the unit circle by $|\det(J)| = 1$. It is possible to get a bifurcation depending on the other properties. Inequalities become equals in the following ways:

$$1 - \mathrm{tr}(J) + \det(J) = 0, \quad \text{or} \quad 1 + \mathrm{tr}(J) + \det(J) = 0.$$

The trace is:

$$\mathrm{tr}(\tilde{J}) = (1 + h(-1 + s)) + (1 - hr) = 2 + h(s - r - 1).$$

The determinant is:

$$\begin{aligned} \det(\tilde{J}) &= (1 + h(-1 + s))(1 - hr) + h^2 sr \\ &= (1 - h + hs)(1 - hr) + h^2 sr \\ &= (1 - h)(1 - hr) + hs(1 - hr) + h^2 sr \\ &= (1 - h)(1 - hr) + hs \\ &= 1 - hr - h + h^2 r + hs \\ &= 1 - h(1 + r) + h^2 r + hs \end{aligned}$$

Thus,

$$\boxed{\det(\tilde{J}) = 1 - h(1 + r) + h^2 r + hs}.$$

and

$$\boxed{\mathrm{tr}(\tilde{J}) = 2 + h(s - r - 1)}.$$

Substitute the symbolic forms:

$$\begin{aligned} \mathbf{SC}_1 &\Leftrightarrow 1 - [2 + h(s - r - 1)] + \left[1 - h(1 + r) + h^2 r + hs\right] > 0, \\ \mathbf{SC}_2 &\Leftrightarrow 1 + [2 + h(s - r - 1)] + \left[1 - h(1 + r) + h^2 r + hs\right] > 0, \\ \mathbf{SC}_3 &\Leftrightarrow \left|1 - h(1 + r) + h^2 r + hs\right| < 1. \end{aligned}$$

These inequalities define a region in the parameter space (α, β, ρ, h) for which the fixed point is locally asymptotically stable.

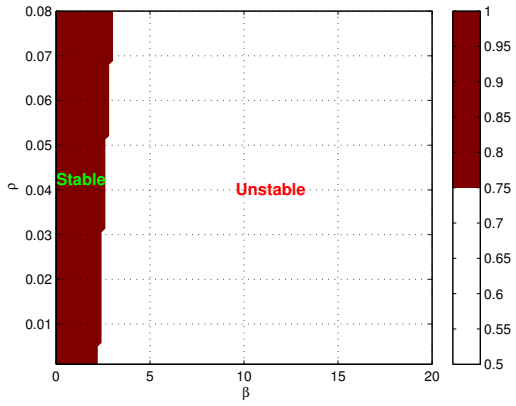

(a) (β, ρ) plane

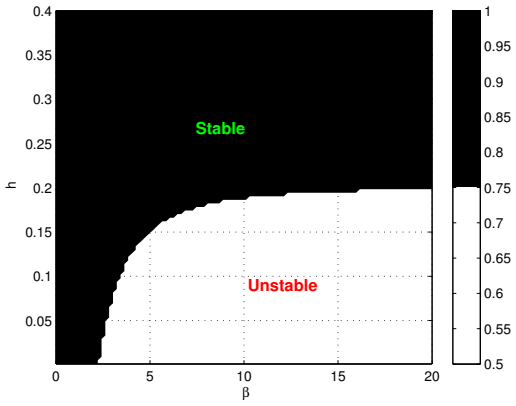

(b) (β, h) plane

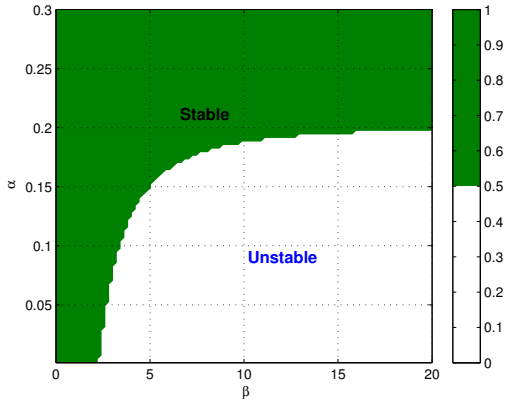

(c) (β, α) plane

Figure 1 Illustration of stability regions: (a) (β, ρ) with $\alpha = 0.3$ and $h = 0.4$ (1a), (b) (β, h) with $\alpha = 0.3$ and $\rho = 0.08$ (1b), and (c) (β, α) with $h = 0.4$ and $\rho = 0.08$ (1c). In all cases, β varies from 1 to 20.

CHAOS CONTROL

In this section, we examine chaos control via state feedback (Elaydi 2005; Abbas and Khaliq 2023). First, we will discuss marginal stability for completeness.

Definition 2. In a marginally stable system, neither stability nor instability are present, but just exist between them. Small perturbations have the potential to make an unstable system.

We have the following discrete biological model (4):

$$\left.\begin{aligned} x_{n+1} &= x + h\left(\alpha - x + \frac{x^2 y}{1+\rho x^2}\right) \\ &\quad - p(x-\alpha-\beta) \\ &\quad - q\left(y - \frac{\beta+\alpha^2\beta\rho+2\alpha\beta^2\rho+\beta^3\rho}{(\alpha+\beta)^2}\right), \\ y_{n+1} &= y + h\left(\beta - \frac{x^2 y}{1+\rho x^2}\right) \end{aligned}\right\} \tag{11}$$

Control is added by the addition of

$$w_n = -p(x-\alpha-\beta) - q\left(y - \frac{\beta+\alpha^2\beta\rho+2\alpha\beta^2\rho+\beta^3\rho}{(\alpha+\beta)^2}\right)$$

, with p, q indicating feedback gains. The following map is used to evaluate the variational matrix J_P at the interior fixed point P:

$$(G, H) \longmapsto (x_{n+1}, y_{n+1}) \tag{12}$$

Where

$$\left.\begin{aligned} G: &= x + h\left(\alpha - x + \frac{x^2 y}{1+\rho x^2}\right) \\ &\quad - p(x-\alpha-\beta) \\ &\quad - q\left(y - \frac{\beta+\alpha^2\beta\rho+2\alpha\beta^2\rho+\beta^3\rho}{(\alpha+\beta)^2}\right), \\ H: &= y + h\left(\beta - \frac{x^2 y}{1+\rho x^2}\right) \end{aligned}\right\} \tag{13}$$

$$J_P = \begin{pmatrix} 1 - p + h\left(-1 - \frac{2kx^3y}{(1+kx^2)^2} + \frac{2xy}{1+kx^2}\right) & -q + \frac{hx^2}{1+kx^2} \\ h\left(\frac{2kx^3y}{(1+kx^2)^2} - \frac{2xy}{1+kx^2}\right) & 1 - \frac{hx^2}{1+kx^2} \end{pmatrix}$$

λ_1, λ_2 represent the characteristic root of J_P at P, then

$$\begin{aligned} \lambda_1 + \lambda_2 = &- \frac{1}{\alpha+\beta+(\alpha+\beta)^3\rho}\Big[\alpha^3\left(h(1+\rho)+\rho(-2+p)\right) \\ &+ 3\alpha^2\beta\left(h(1+\rho)+\rho(-2+p)\right) \\ &+ \beta\left(h(-1+\beta^2(1+\rho))+(1+\beta^2\rho)(-2+p)\right) \\ &+ \alpha\left(h(1+3\beta^2(1+\rho))+(1+3\beta^2\rho)(-2+p)\right)\Big] \end{aligned} \tag{14}$$

$$\begin{aligned} \lambda_1 \cdot \lambda_2 = &\frac{1}{\alpha+\beta+(\alpha+\beta)^3\rho}\Big[\alpha(-1+3\beta^2(h-\rho))(-1+h+p) \\ &+ \alpha^3(h-\rho)(-1+h+p) \\ &+ 3\alpha^2\beta(h-\rho)(-1+h+p) \\ &+ \beta\Big(\beta^2h^2 - (1+\beta^2\rho)(-1+p) \\ &- h\left(-1+\beta^2(1+\rho-p)+2q\right)\Big)\Big] \end{aligned} \tag{15}$$

According to equations (14) and (15), marginal stability lines can be found ($\lambda_1 = \pm 1$ and $\lambda_1\lambda_2 = 1$). It ensures that the moduli of the eigenvalues are less than 1.

When $\lambda_1\lambda_2 = 1$, then from Eq. (14), we can get

$$\begin{aligned} L_1: = &\frac{\alpha(-1+3\beta^2(h-\rho))+\alpha^3(h-\rho)+3\alpha^2\beta(h-\rho)}{\alpha+\beta+(\alpha+\beta)^3\rho}(-1+h+p) \\ &+ \frac{\beta\left(\beta^2h^2-(1+\beta^2\rho)(-1+p)-h\left(-1+\beta^2(1+\rho-p)+2q\right)\right)}{\alpha+\beta+(\alpha+\beta)^3\rho} - 1 = 0 \end{aligned} \tag{16}$$

When $\lambda_1 = 1$, then from Eq. (13) and Eq. (14), we can get

$$L_2: \frac{(\alpha+\beta)^3h(h+p)-2\beta hq}{\alpha+\beta+(\alpha+\beta)^3\rho} = 0 \tag{17}$$

When $\lambda_1 = -1$, then from Eq. (13) and Eq. (14), we can get

$$\begin{aligned} L_3: = &\frac{\alpha(-2+3\beta^2(h-2\rho))+\alpha^3(h-2\rho)+3\alpha^2\beta(h-2\rho)}{\alpha+\beta+(\alpha+\beta)^3\rho}(-2+h+p) \\ &+ \frac{\beta\left(\beta^2h^2-2(1+\beta^2\rho)(-2+p)+h\left(2+\beta^2(-2-2\rho+p)-2q\right)\right)}{\alpha+\beta+(\alpha+\beta)^3\rho} = 0 \end{aligned} \tag{18}$$

The triangular region obtained by combining equations (16), (17) and (18) reveals that $|\lambda_{1,2}| < 1$.

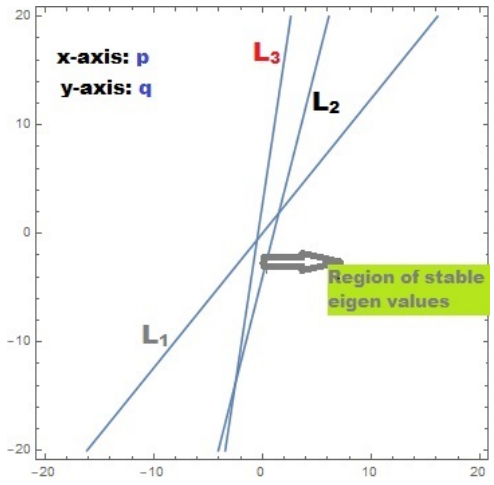

Figure 2 Region of stability where $|\lambda_{1,2}| < 1$

NUMERICAL ANALYSIS

Using the bifurcation parameter range $\beta \in [1, 20]$, we carried out a detailed numerical analysis of the system (4). There is a complex pattern of dynamic transition as shown in Figure 3. It exhibits a stable fixed point starting at a low value of $\beta = 1$ and gradually increasing up to $\beta \approx 2$. There is a steady state for both x_n and y_n on account of the convergence of their trajectories. In response to increasing β, particularly at $\beta \approx 3{-}4$, the fixed point destabilizes, giving rise to periodic behavior through the classical period-doubling bifurcation, leading to stable 2-cycles and eventually 4-cycles. A chaotic dynamic is observed as the system progresses upward between approximately $\beta = 6$ to $\beta = 9$. It is characterized by irregular, non-repeating patterns and a strong dependence on initial conditions. Periodic windows interrupt the chaotic region, such as around $\beta \approx 6.7$, where the system temporarily returns to a stable periodic orbit before re-entering chaos. After $\beta = 10$, this periodic-chaotic pattern continues. The

behavior becomes chaotic once again in the interval $\beta = 16-19$ following regular cycles in the interval $\beta = 13-15$.

Specifically, the system (4) in $\beta \in [1, 20]$ demonstrates a delicate interaction between periodicity, stability, and chaos. The numerical simulations captured in Figures 3 and 4 provide a compelling visualization of this bifurcation structure.

In order to control the chaotic behavior of the system (4), we have used the state feedback control method. To verify the validity of our results, we will proceed to Section (4). The values of $\alpha = 0.3$, $h = 0.4$, $\rho = 0.08$ and $\beta = 3.18$ can be used to obtain (15), (16), and (17).

$$L_1: = -1 + 0.145953\Big(2.89576(-0.6+p) + 3.18\Big(1.61798 - 1.80899(-1+p) - 0.4\big(-1 + 10.1124(1.08-p) + 2q\big)\Big)\Big) = 0 \tag{19}$$

$$L_2: \; 0.145953\big(16.8577(0.4+p) - 2.544q\big) = 0 \tag{20}$$

$$L_3: = 0.145953\Big(1.79682(-1.6+p) + 3.18\Big(1.61798 - 3.61798(-2+p) + 0.4\big(2 + 10.1124(-2.16+p) - 2q\big)\Big)\Big) = 0 \tag{21}$$

Equations (19), (20), and (21) describe lines that intersect to form a triangular region corresponding to $|\Lambda_{1,2}| < 1$, as shown in Figure 2.

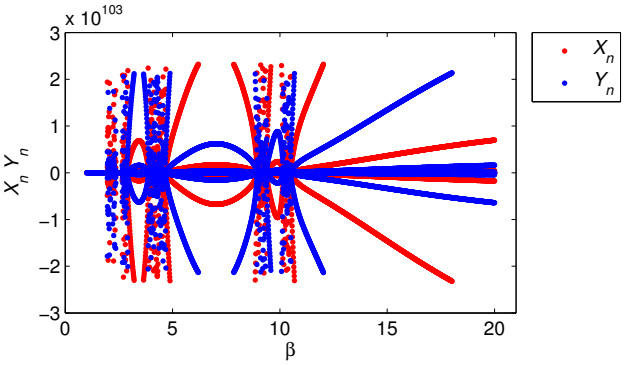

Figure 3 Bifurcation diagram of the system (4) showing the variation in x_n (red) and y_n (blue) w.r.t bifurcation parameter β. The diagram captures transitions from stability to chaos and divergence.

GLOBAL BIFURCATION OVERVIEW FOR $\beta \in [1, 100]$

The bifurcation structure of system (4) reveals intricate and diverse dynamical behavior as the bifurcation parameter β ranges from 1 to 100. As illustrated in Figure 5, the system undergoes a series of transitions among stable states, periodic oscillations, and chaotic regimes, depending on the value of β. This diagram captures the long-term evolution of the system's state variables, highlighting the sensitivity and richness of its nonlinear dynamics.

Table 2 shows that system (4) does not exhibit a monotonic transition from stability to chaos over the interval $\beta \in [1, 100]$. Instead, the dynamics follow the sequence:

$$\text{Stable} \to \text{Cyclic} \to \text{Chaotic} \to \text{Periodic window} \to \text{Chaotic} \to \text{Unstable}.$$

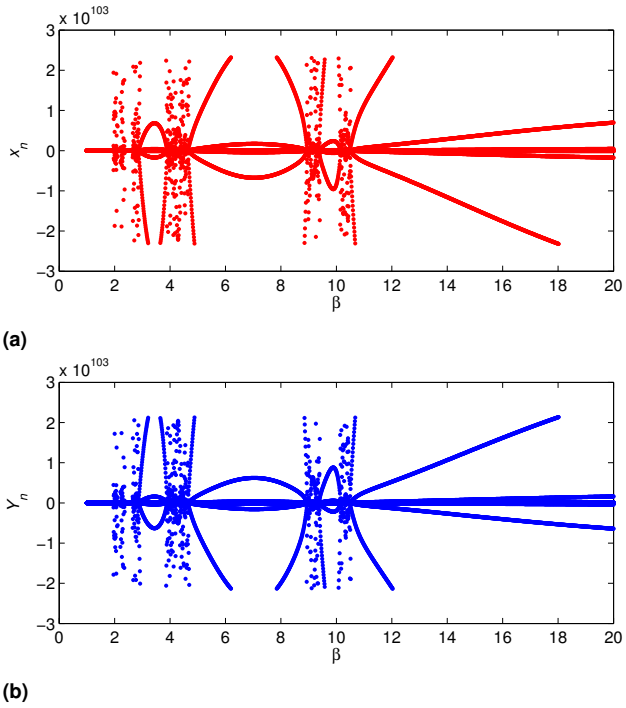

Figure 4 Bifurcation diagrams of system (4) with respect to the bifurcation parameter β: Figure 4a shows transitions in x_n , while Figure 4b shows transitions in y_n. The diagrams capture the progression from stability to chaos and eventual divergence.

Table 2 Dynamical behavior of the system as β varies

Interval for β	Behavior Type	Description
1−2, 10−12, 20−22	Point of stability	The system reaches an equilibrium state when both x_n and y_n converge.
3−4, 13−15, 23−25	Doubling the period	Onset of periodic oscillations with 2-cycles and 4-cycles as the fixed point becomes unstable.
6−9, 16−19, 26−30	Dynamics of chaos	Evolution dominated by irregular, non-repeatable trajectories dependent upon the initial conditions.
$\sim$ 38, 48, 68	Periodic windows	Regular cycles reappear within chaotic regimes (e.g., period-3, period-6), indicating pockets of order.
> 90	Divergent/Unstable	Unlimited growth; trajectories may diverge or exhibit instability beyond attractor boundaries.

The recursive dynamics of system (4) arise from its inherent non-linearity and saturated feedback structure. As the parameter β increases, the system exhibits growing sensitivity to parameter changes. This behavior is visually captured in the bifurcation diagram shown in Figure 5, which clearly marks the onset of bifur-

cations and the progressive emergence of complex dynamics from initially simple evolution rules.

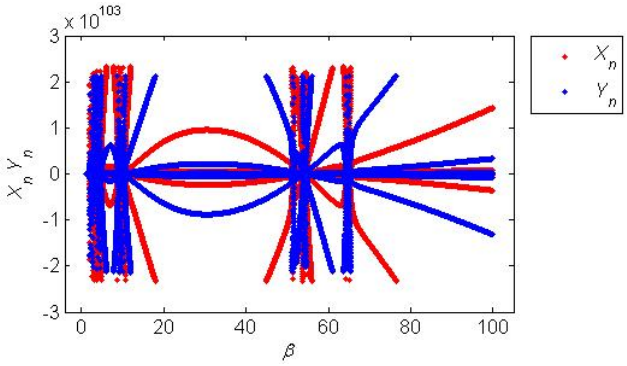

Figure 5 Bifurcation diagram of the system (4) displaying the long-term behavior of x_n (red) and y_n (blue) as the bifurcation parameter β varies over the interval $[1, 100]$. The diagram highlights the onset of complex dynamics, including period-doubling bifurcations, multistability, and chaotic oscillations induced by substrate inhibition effects.

COMPARATIVE DISCUSSION WITH THE CLASSICAL SEL'KOV MODEL

The classical Sel'kov model, formulated in continuous time as a system of ordinary differential equations (ODEs), has been extensively studied as a minimal model for glycolytic oscillations. It is known for its ability to capture sustained oscillations via Hopf bifurcations and its relatively simple nonlinear structure, which has made it a benchmark in biochemical dynamics studies. However, the original formulation lacks explicit mechanisms for inhibitory feedback, a limitation when modeling biochemical systems in which enzyme activity is reduced at high substrate concentrations.

In this work, we have developed a discrete-time variant of the Sel'kov model that explicitly incorporates substrate inhibition through nonlinear feedback terms. This modification is motivated by biological observations of saturation effects in enzymatic reactions, particularly in systems regulated through pulse-like inputs, switch-like transitions, or temporally sampled external control. The discrete formulation allows for a natural representation of such regulatory mechanisms and provides a framework for analyzing the interplay between time discretization and nonlinear biochemical feedback.

To facilitate a direct comparison between the two approaches, we summarize the key differences in Table 3. The comparison covers model formulation, biological interpretation, dynamical behavior, stability analysis, and the use of chaos control techniques.

The comparison highlights clear distinctions between the two formulations. The discrete Sel'kov model extends the classical framework by incorporating an inhibitory feedback mechanism absent in the continuous counterpart, broadening applicability to systems where inhibition is biologically relevant. This addition enriches the dynamical repertoire, allowing phenomena such as period-doubling cascades and chaotic regimes behaviors unattainable in the original model, which is limited to Hopf-induced oscillations. Stability requirements also differ: the continuous model demands eigenvalues with negative real parts, whereas the discrete form relies on the Schur–Cohn condition, making stability more sensitive to discretization step size and parameter variations. Furthermore, the discrete framework enables direct chaos-control

Table 3 Comparison between the classical continuous-time Sel'kov model and the proposed discrete-time Sel'kov model with substrate inhibition

Aspect	Classical Continuous Sel'kov Model	Proposed Discrete Sel'kov Model with Substrate Inhibition
Model Formulation and Mechanism		
Mathematical Formulation	ODE system without inhibitory terms in the reaction kinetics.	Discrete-time system incorporating nonlinear substrate inhibition directly in the reaction terms.
Biological Representation	Captures continuous metabolic flows; assumes no enzyme inhibition.	Represents saturation effects and enzyme inhibition; suited for pulse-like or discrete regulatory mechanisms.
Dynamical Behavior		
Typical Dynamics	Stable fixed points; oscillations via Hopf bifurcation.	Rich dynamics including bifurcation cascades, chaotic windows, and marginal stability zones.
Bifurcation Features	Hopf bifurcations produce stable limit cycles for specific parameters.	Period-doubling route to chaos as β increases ($\alpha = 0.3$, $h = 0.4$, $\rho = 0.08$).
Stability Analysis		
Criterion	Stability if all Jacobian eigenvalues have negative real parts.	Stability via Schur–Cohn criterion: eigenvalues must lie inside the unit circle; sensitive to step size and parameter changes.
Control and Applications		
Chaos Control	Typically not addressed in the literature.	Linear state feedback control stabilizes chaotic trajectories ($\beta = 3.18$).
Biological Relevance	May miss discrete regulatory effects such as switching or pulse signaling.	Well-suited for modeling time-sampled regulation and discrete biochemical events.

strategies; for example, linear state feedback can stabilize chaotic trajectories and restore fixed-point behavior in marginally stable regimes, offering practical regulation methods for synthetic biochemical systems. Biologically, the discrete model better captures processes with inherently discrete operation such as periodic forcing, signal gating, or digital biochemical circuits—while the continuous model, though effective for smooth flows, lacks inhibitory representation and cannot model saturation-driven nonlinearities. Overall, the discrete Sel'kov model with substrate inhibition offers a more versatile and insightful framework for exploring complex dynamics and implementing control strategies in nonlinear biochemical systems where discrete regulation and inhibition are central. Incorporating substrate inhibition, which reduces enzyme activity at high substrate levels, gives the model a more realistic enzymatic regulation and overcomes a key limitation of the classical Sel'kov model.

CONCLUSION

We established and studied a discrete-time model by modifying Sel'kov glycolysis with a nonlinear feedback saturation term incorporating substrate inhibition. By accounting for regulatory mechanisms frequently observed in enzymatic reactions, this modification enhances the model's biological relevance, while the discrete-time formulation allows for an examination of dynamics under

iterative updates, which is particularly relevant for numerical simulations and biological pulsed systems. This study exclusively utilizes the proposed discrete-time model for its analytical and numerical results. The chaotic dynamics were observed in the system (4) with parameter values of $\alpha = 0.3$, $h = 0.4$, and $\rho = 0.08$, with bifurcation parameter β in the range $[0, 20]$, as a cascade of period-doubling bifurcations occurred. There are classical routes to chaos in discrete nonlinear systems, and these transitions suggest our model captures deeper dynamics than simple fixed points. Further, we successfully applied the state feedback strategy to control the chaotic behavior of the proposed system, as shown in Figure-2 . Despite our reference to the continuous-time Sel'kov model to explain Hopf bifurcations and limit cycles, we did not include any simulations or results from the unmodified Sel'kov model. There is no period-doubling route to chaos within the continuous model, unlike discrete dynamics. Thus, the comparison highlights the novel behaviors introduced by our feedback mechanism and discrete-time formulation.

Additionally, we demonstrated chaos control with our model. Specifically, the system can be stabilized at its unique fixed point by appropriate parameter tuning at $\beta = 3.18$, which lies within a region of marginal stability. This result showcases the potential for implementing simple yet effective control strategies in discrete biochemical systems where oscillatory or chaotic behaviors may be undesirable. Although no new experiments were conducted, the model's oscillatory and chaotic behaviors align with reported glycolytic oscillations, suggesting it captures dynamics relevant to real biochemical systems. Overall, the discrete-time model with substrate inhibition offers a robust and flexible framework to explore nonlinear behaviors in biochemical systems. By preserving basic dynamics of the classical Sel'kov model, it introduces new phenomena that are relevant to both theoretical and applied studies, such as period-doubling bifurcations and controllable chaos. Developing hybrid models that integrate continuous metabolic dynamics with discrete regulatory mechanisms may enhance the model's applicability in systems biology and synthetic biochemical circuit design in the future.

Future extensions may improve the model's representation of biological systems. These include introducing stochastic fluctuations to capture random variability, linking multiple oscillators to study coordinated dynamics, or incorporating stochastic enzyme kinetics to reflect molecular-level variability. Such developments would provide deeper insight into complex biochemical behaviors and expand the model's potential applications in systems biology and synthetic circuits.

Acknowledgments

There is no specific funding assigned to this research.

Ethical standard

The authors have no relevant financial or non-financial interests to disclose.

Availability of data and material

All data used in this manuscript are properly cited.

Conflicts of interest

The authors declare that there is no conflict of interest regarding the publication of this paper.

LITERATURE CITED

Abbas, A. and A. Khaliq, 2023 Analyzing predator–prey interaction in chaotic and bifurcating environments. Chaos Theory and Applications **5**: 207–218.

Alligood, K. T., T. D. Sauer, and J. A. Yorke, 1996 *Chaos: An Introduction to Dynamical Systems*. Springer, New York.

Bastin, G. and D. Dochain, 1990 *On-line Estimation and Adaptive Control of Bioreactors*. Elsevier, Amsterdam.

Bertram, R., L. S. Satin, M. Zhang, P. Smolen, and A. Sherman, 2007 Metabolic and electrical oscillations: partners in controlling pulsatile insulin secretion. American Journal of Physiology-Endocrinology and Metabolism **293**: E890–E900.

Chen, L., R. Wang, and K. Aihara, 2021 Nonlinear dynamical systems in biology: Analysis and control. Annual Review of Biomedical Engineering **23**: 75–106.

De Vries, G., T. Hillen, M. Lewis, J. Muller, and B. Schonfisch, 2006 *A Course in Mathematical Biology: Quantitative Modeling with Mathematical and Computational Methods*. SIAM, Philadelphia.

Elaydi, S., 2005 *An Introduction to Difference Equations*. Springer, New York, third edition.

Fall, C. P., E. S. Marland, J. M. Wagner, and J. J. Tyson, 2002 *Computational Cell Biology*. Springer, New York.

Gambino, G., M. C. Lombardo, and M. Sammartino, 2022 Discrete dynamical modeling of ecological and biological systems. Mathematics **10**: 1154.

Gaspers, L. D. and A. P. Thomas, 2000 Mitochondrial metabolism of pyruvate is required for glucose-stimulated insulin secretion and is regulated by calcium in β-cells. Molecular and Cellular Endocrinology **167**: 1–10.

Glass, L. and M. C. Mackey, 1988 *From Clocks to Chaos: The Rhythms of Life*. Princeton University Press, Princeton.

Goldbeter, A., 1996 *Biochemical Oscillations and Cellular Rhythms: The Molecular Bases of Periodic and Chaotic Behaviour*. Cambridge University Press, Cambridge.

Guckenheimer, J. and P. Holmes, 1983 *Nonlinear Oscillations, Dynamical Systems, and Bifurcations of Vector Fields*. Springer, New York.

Hassard, B. D., N. D. Kazarinoff, and Y.-H. Wan, 1981 *Theory and Applications of Hopf Bifurcation*. Cambridge University Press, Cambridge.

Heinrich, R. and S. Schuster, 1996 *The Regulation of Cellular Systems*. Springer, New York.

Hofmeyr, J.-H. S. and A. Cornish-Bowden, 1986 The thermodynamic basis of metabolic control analysis. European Journal of Biochemistry **155**: 265–270.

Kuznetsov, Y. A., 2004 *Elements of Applied Bifurcation Theory*. Springer, New York, third edition.

Merdan, H. and O. Duman, 2022 Stability and period-doubling bifurcation in a modified commensal symbiosis model with allee effect. Mathematical Modelling of Natural Phenomena **17**: 1–16.

Murray, J. D., 2002 *Mathematical Biology I: An Introduction*. Springer, New York, third edition.

Nicolis, G. and I. Prigogine, 1977 *Self-Organization in Nonequilibrium Systems: From Dissipative Structures to Order through Fluctuations*. Wiley, New York.

Richard, P., 2003 Metabolic regulation: a precision-control mechanism of the cell. Biochemical Journal **375**: 1–16.

Sataric, M. V., T. Nemes, and J. A. Tuszynski, 2024 Re-examination of the sel'kov model of glycolysis and its symmetry-breaking instability due to diffusion. Biophysica **4**: 545–560.

Schnakenberg, J., 1979 Simple chemical reaction systems with limit cycle behaviour. Journal of Theoretical Biology **81**: 389–400.

Segel, L. A., 1988 *Modeling Dynamic Phenomena in Molecular and Cellular Biology*. Cambridge University Press, Cambridge.

Sel'kov, E. E., 1968 Self-oscillations in glycolysis: I. a simple kinetic model. European Journal of Biochemistry **4**: 79–86.

Strogatz, S. H., 2015 *Nonlinear Dynamics and Chaos: With Applications to Physics, Biology, Chemistry, and Engineering*. CRC Press, Boca Raton, second edition.

Teusink, B. *et al.*, 2000 Can yeast glycolysis be understood in terms of in vitro kinetics of the constituent enzymes? testing biochemistry. European Journal of Biochemistry **267**: 5313–5329.

Tornheim, K. and J. M. Lowenstein, 1979 Oscillations of glycolysis in yeast: evidence for an atp-initiated feedback system. Proceedings of the National Academy of Sciences of the USA **76**: 6602–6606.

Wiggins, S., 2003 *Introduction to Applied Nonlinear Dynamical Systems and Chaos*. Springer, New York.

Yoshino, M., K. Murakami, and A. Tsuji, 2015 Analysis of the substrate inhibition of complete and partial types. Biochemical and Biophysical Reports **3**: 1–6.

How to cite this article: Abbas, A., and Khaliq, A. Nonlinear Dynamics and Chaos Control in a Discrete Sel'kov Model with Substrate Inhibition. *Chaos and Fractals*, 3(1), 29-37, 2026.